



The correlation between Re and P and their synergetic effect on the rupture strength of the γ -Ni/ γ' -Ni₃Al interface

L. Peng^{a,b}, P. Peng^{b,*}, Y.G. Liu^a, S. He^b, H. Wei^c, T. Jin^c, Z.Q. Hu^c

^a College of Environmental Science and Engineering, Hunan University, Changsha 410082, China

^b School of Material Science and Engineering, Hunan University, Changsha 410082, China

^c Superalloys Division, Institution of Metal Research, CAS, Shenyang 110016, China

ARTICLE INFO

Article history:

Received 7 February 2012

Received in revised form 19 June 2012

Accepted 20 June 2012

Available online 20 July 2012

Keywords:

γ -Ni/ γ' -Ni₃Al interface

Griffith rupture work

Correlative and synergetic effect between alloying and doping elements

First-principles calculation

ABSTRACT

A first-principles investigation on the synergetic effect of Re and P on Griffith rupture works of the γ -Ni/ γ' -Ni₃Al interface is performed. The calculated results indicate site preference of P at the γ/γ' interface is not changed by Re-addition but P-induced embrittlement can be inhibited even reversed by the addition of Re at the adjacent atomic layer of P. The correlative effect between P and Re at the γ/γ' interface is also evaluated by a correlative energy function. It is found a strong repulsive interaction between P-doping and Re-addition is limited within a unit cell of γ or γ' phase and is not profitable for the strengthening of the γ/γ' interface. The electronic and geometric structures reveal a large interfacial separation and the depletion of electron densities in the interfacial region should be responsible for the potential inter-phase cleavage fracture site, and the deleterious effect of P can be attributed to a mutual influence of local elastic strain energy and atomic bonding energy in the doped system.

© 2012 Elsevier B.V. All rights reserved.

1. Introduction

Ni-based single crystal (SC) superalloys are one of the key structural materials for high-temperature applications in the advanced aeroengines and gas turbines. The remarkable high-temperature mechanical properties of Ni-based SC superalloys are primarily due to their unique microstructures, containing a high volume fraction of intermetallic γ' -Ni₃Al precipitates (L1₂ structure) embedded coherently in a FCC γ -Ni matrix. In-service examination and failure analyses have shown that the structure and properties of the γ/γ' interface have a great influence on the shape, size and coarsening rate of γ' precipitates which in return strongly affect the creep strength or creep rupture life of Ni-based SC superalloys subjected to stress at elevated temperatures [1]. Another important impact on high-temperature mechanical properties of Ni-based SC superalloys is given by the solid solution strengthening of the γ -matrix, in which Re is well known to be favorable to improve the creep resistance and high temperature capability [2–4]. However, the subsequent increase of Re from 3 wt.% in the second generation to 6 wt.% in the third generation raises the susceptibility to formation of brittle and deleterious topologically close packed (TCP) phases. This long-term phase stability problem leads to an addition of Ru or Ir in the latest generation of Ni-based SC superalloys [5].

Many experiments have demonstrated that trace elements and minor alloying additions, e.g., N, O, H, S, P, Si, As, Se, C, B, etc., have a great influence on the strength and ductility of Ni-based SC superalloys [6]. Phosphorus used to be recognized as a deleterious trace element, which must be strictly controlled in Ni-based SC superalloys. Phosphorus seriously segregates to the grain boundary of γ and γ' phases and then leads to the cohesive strength of grain boundaries to be weakened [7]. However, a big breakthrough has been made recently on the beneficial effect of P in some wrought superalloys, e.g., GH761 and IN718 superalloy [8]. It is found the stress-rupture life of commercial GH761 alloy at 650 °C and 637 MPa increased quickly if the phosphorus content rose up from 0.0005 wt.% to 0.016 wt.%, and then dropped down beyond the limited amount. A same advantageous effect was also detected in IN718 alloy, in which the phosphorus content was 0.022 wt.% corresponding to the peak life at 649 °C. Unlike Boron segregation at the grain boundaries of γ' phases and the γ/γ' interface [9–11], the occupation behavior of P at the γ -Ni/ γ' -Ni₃Al interface and its effect on interfacial properties are scarcely reported in the literature [12]. Hence an in-depth and thorough understanding of site preference of P-doping and its roles on strength and toughness of the γ/γ' interface is desired in order to guide the control of trace elements and minor alloying additions in Ni-based SC superalloys.

As well-known, the partitioning and segregation behavior of additions and dopants have a critical role on the cohesive properties of the γ/γ' interface of Ni-based SC superalloys. To understand the site preference of alloying and doping elements, several

* Corresponding author.

E-mail address: ppeng@hnu.edu.cn (P. Peng).

investigations have been done in ternary γ - γ' dual phase model alloys even commercial superalloys. Using Atomic Site Location by CHannelling Enhanced Microanalysis (ALCHEMI), Ofori et al. [13] examined the site preference of Ru in a ternary Ni-19at.%Al-3at.%Ru alloy and found 60at.% of Ru to situate at Al sites in γ' -phase. Kitashima et al. [14] further examined the effect of alloying content on the equilibrium segregation at and adjacent to the γ/γ' interface by the Cluster Variation Method incorporated with the tetrahedron approximation and the phenomenological Lennard-Jones potential. The obtained results suggested Al-site occupiers in the γ' -phase such as Mo, Re and W would be enriched on the side of the γ -phase near by the γ/γ' interface. By atom-probe tomography (APT) combining with first-principles calculation, Seidman et al. [15–17] investigated the partitioning and segregation behavior of Cr, Ta, Re, Ta, W, Hf, Ru in several model superalloys. Both Re and Ru were found to partition to γ -phase, and prefer to occupy Al sites in γ' -phase [16]. Although W and Cr partitions preferentially to the γ' -phase in a ternary Ni-Al-W/Cr alloy, its partitioning behavior is reversed in favor of the γ -phase in multi-component alloys. Furthermore, the degree of W- or Cr-partitioning to the γ' -phase decreases with the addition of Ta to a Ni-Al-Cr/W-Ta alloy due to a strong Al site preference of Ta than Cr and W [15,17–18]. Similarly, the partitioning behaviors of W and Mo in the γ and γ' phases could be also affected by the site preference of Re and Ru at the γ/γ' interface [19]. In this case, a strong Cr-partitioning to the γ -phase even causes a reversal Hf-partitioning to the γ -phase because of a strong attractive interaction between Hf and Cr atoms [20]. No evidence indicated Re formed solute clusters above the level expected from random fluctuations in CMSX-4 superalloys [21]. And the enrichment of Re in γ -phase matrix was detected to be close to the γ/γ' interface. The work of Zhu et al. [22] further suggested the distribution of Re near by the γ/γ' interface in Ni-based SC superalloys has two kinds of types after creep tests. One is in γ phases; the other is close to the dislocation cores. The enrichment of Re near the dislocation cores was considered to be profitable for the improvement of high-temperature performances of Ni-based SC superalloys due to its restraint function to dislocation movement. A molecular dynamics (MD) simulation showed both γ phases and γ/γ' interfaces could be stabilized by the addition of Re, and Re-addition could significantly affect the degree of mismatch between γ and γ' phases [23]. However, deferent from the observation of Reed et al. [21], the MD simulation showed Re atoms had a tendency to cluster in both γ and γ' phases. And either at Ni sites in γ phase or at Al sites in γ' phase, the substitution Re for host atoms could distinctly enhance the bonding strength between Re and its first nearest neighbor (FNN) host atoms, therefore it is favorable to inhibit the dislocation motion along the γ/γ' interface [23].

Since experimental techniques are still limited for detecting trace impurities at the γ -Ni/ γ' -Ni₃Al interface, a sole option is the quantum-mechanism theoretical calculation [24] based on density functional theory (DFT). By means of cluster models and a DV-X α method, Wu et al. [25] firstly investigated the segregation behavior of B and H in Ni-based and Ni₃Al-based alloys. The results showed both B and H may segregate to the octahedral interstices in the Ni/Ni₃Al interface but boron has a greater segregation tendency and higher stability than hydrogen. Latterly, Sanyal et al. [26] further investigated the site preference of O, H and N at the Ni/Ni₃Al interface and estimated their effects on the interfacial cleavage energy with the help of *ab initio* VASP software. They found that O and H have intrinsic tendencies to segregate to the octahedral interstice constituted by 6 Ni atoms in the interfacial region. Our recent work [27] on the probability of S-doping and its site preference in the γ -Ni/ γ' -Ni₃Al interfacial region also indicated that S-doping is energetically permissible either at sub-lattice sites or at octahedral interstitial centers, and S atoms prefer to substitute host atoms,

especially Ni atoms at the coherent (002) interfacial atomic layer. However, among octahedral interstitial centers, the most favorable situation is S to segregate to an octahedral interstice bounded by 6 Ni atoms at the coherent interfacial layer rather than the interstice octahedron consisting of 5 Ni and 1 Al atoms [28].

In the past decades, an increasing experimental and theoretical investigation on strengthening effects of alloying elements in Ni-based SC superalloys was also reported. Using the molecular orbital DMol3 package, Chen et al. [29] examined the alloying influence of substitutional elements (Mo, V, Nb, W, Ti, Re, Cr, Ta, Hf, Ru, Ir, Rh, Al) at the γ/γ' interface of Ni-based SC superalloys. The charge density difference indicated a strong anisotropic bonding formed between the alloying element and its FNN host Ni atoms due to *d-d* hybridization. By a local sum of horizontal and vertical Mayer bond orders and their ratio, i.e., $\sum BO^h/\sum BO^v$, they characterized and evaluated the competition between the shear and cohesive strengths as well as the embrittlement trend of the γ/γ' interface, and found W-addition is the most beneficial for the improvement of the creep rupture strength. The investigation on the synergetic effect of Re and Ru on the γ/γ' interfacial strengthening showed the duplex addition of Re and Ru was better than any individual addition of Re or Ru due to the *d* orbit hybridization and the charge transfer among Re, Ni and Ru atoms [30]. Ning et al. [31] investigated strengthening effects of Re, Ru, Cr, Co, W, Ta at the γ/γ' interface in terms of the Griffith work and suggested the substitution of Re for Ni at the coherent interfacial layer was the most advantageous [32]. Wang et al. [33] studied the optimal geometries and mechanical properties of the γ/γ' interface with Re- or Ru-addition in the framework of DFT. The calculated results on the basis of the brittle cleavage and the generalized stacking fault energies indicated both substitutions of Re and Ru for Al in γ' -phase could enhance the coherent strength of the γ/γ' interface, but Re-addition was more effective than Ru-addition. For the improvement of tensile and shear strengths of γ' -phase caused by strong Re-Ni covalent-like bonding [34], a thermodynamic explanation was that Re-addition inhibited the formation of Ni-vacancies and prohibited the migration of neighboring vacancies but facilitated to form Al-vacancies [35]. All these findings clearly indicate the binding strength of the γ/γ' interface can be improved by addition of Re or Ru.

In addition to additions of alloying elements, a series of doping of trace and minor elements in Ni-based SC superalloys were also investigated. These impurities and trace elements, such as B, C, N, H, O, P and S, have a great influence on the mechanical properties of Ni-based SC superalloys [12,24,28], among which B is regarded as a typical enhancer. B can improve the cohesive strength of grain boundaries [9,10] and reduce the embrittlement effect of H [9,11] because of its strong tendency to segregate to grain boundaries of γ' phases, which leads to a local disordering in the grain boundary region and a strong interaction with adjacent γ phase. By contrary, O is generally considered as a deleterious dopant for the improvement of the ductility of Ni- or NiAl-based alloys due to the formation of the covalent component containing Al₂O₃-like tetrahedron structure in the bulk or a coplanar O-Al cluster in the grain boundary [36,37]. With respect to Ni-based SC superalloys, Liu et al. [24] first investigated the doping effect of the Ni/Ni₃Al interface by a DV-X α method, and found the binding strength of the doped interfaces gradually decreased in the following order: C, B, N, O, H, clean, P, S. Subsequently, Wu et al. [25] revealed B-induced ductility and H-induced embrittlement mainly originated from a different lattice misfit between γ and γ' phases. By a supercell model and VASP software, Sanyal et al. [26] further investigated the influence of O, N and H on the rupture strength of the Ni/Ni₃Al interface. However, different from the embrittlement order suggested by Liu et al. [24] in terms of the binding strength of cluster interfacial models, a careful calculation

of Griffith rupture work showed that O has the most deleterious effect on interfacial toughness, followed by N and H. In fact, a systematic investigation on shear deformation of the TiAl/Ti₃Al interface is also demonstrated the present of O-doping will cause embrittlement of dual phase TiAl–Ti₃Al alloys [38,39]. By the first-principles plane-wave pseudopotential method and CASTEP program, Peng et al. [12] also investigated the effect of B and P on Griffith rupture work and local toughness of the γ/γ' interface and revealed that B is beneficial to the improvement of the interfacial fracture strength, while P has a deleterious effect. Furthermore, Chen et al. [28] have performed a first-principles calculation on the bonding characteristics of S-doped Ni/Ni₃Al interface by means of a molecular orbital DMol package. Their results indicated that a strong bonding between S and Ni atoms lying within the interface, which leads to an increase in the shear strength of the interface over the cohesive strength, is responsible for S-induced embrittlement of the Ni/Ni₃Al interface. Sulfur makes $R_{BO} = \sum BO^h / \sum BO^v$ increases by 121% relative to the S-free γ/γ' interface, but an extra substitution of Re for Al at the γ/γ' interface could obviously reduce this R_{BO} value, which means S-induced embrittlement can be relieved by substituting Al by Re at the Ni/Ni₃Al interface.

From above summary, one can see that either for the site preference or for the interfacial binding strength a correlative and synergetic effect between alloying and doping elements can be seen easily at the γ -Ni/ γ' -Ni₃Al interface. However, it is noticed that previous investigation on S-induced embrittlement of the γ -Ni/ γ' -Ni₃Al interface performed by Chen et al. [28] seldom took into account the influence of the atoms far away from the γ/γ' interface on the interfacial bonding strength. And the site preference of doping atoms in the γ/γ' interfacial region was not considered in their cluster model. Therefore, in this paper, a series of Ni/Ni₃Al interfacial supercells with P-doping at various sub-lattice sites and octahedral interstitial centers will be constructed and adopted to evaluate the doping effect on the cleavage energy and local elastic strain energy of the γ/γ' interface. Different from the previous investigation [28], a periodic supercell model, which is proved to be more appropriate for description of the γ/γ' interface than cluster model [32], will be adopted. A particular attention will be paid to the interplay between P-doping and Re-addition and the synergetic effect of P and Re on the rupture work of the γ/γ' interface. Moreover, the variation in the electronic and geometrical structures of the γ/γ' interface cause by synergetic effect of P and Re will be carefully examined as well.

2. Method and model of calculation

Cambridge serial total energy package (CASTEP), a first-principles plane-wave pseudopotential method [40,41] based on DFT, is employed to investigate energetics and electronic structures of γ -Ni/ γ' -Ni₃Al interface with or without dopants. Ultrasoft pseudopotentials [42] represented in reciprocal space with a exchange-correction function of Perdew–Burke–Emzerhof (PBE) form under generalized gradient approximation (GGA) [43] is applied for all elements involved in present models. These pseudopotentials provided in CASTEP package [41] have been tested. Table 1 lists

Table 1
A test of the ultrasoft pseudopotentials of Ni and Al in Ni₃Al.

	Current work	TB-LMTO [44]	AE-LMTO [45]	Expt. [44,45]
Lattice constant (Å)	3.50	3.51	3.55	3.57
Heat of formation (eV/atom)	2.07	2.20	1.94	1.59–1.62
Bulk modulus (MPa)	1.50	1.46	2.10	2.40

the equilibrium lattice constant, the heat of formation, and the bulk modulus of γ' -Ni₃Al phase. It is found a good agreement with experimental data as well as previous calculation results by tight-binding linear muffin-tin orbital (TB-LMTO) [44] and all electron linear muffin-tin orbital (AE-LMTO) [45] methods can be seen.

In our calculations, the cutoff energy of atomic wave functions (PWs), E_{cut} , is set at 300 eV. A finite basis set correction [46] is applied for evaluation of energy and stress. In the calculation of self-consistent field (SCF), the Pulay scheme of density mixing [47] is utilized. All atomic positions in the supercell are optimized by Broyden–Fletcher–Goldfarb–Shanno (BFGS) scheme [48] based on the cell optimization criterion (RMS force of 0.03 eV/Å, RMS stress of 0.05 GPa and RMS displacement of 1.0×10^{-3} Å). The calculation of total energy and electronic structures is followed by cell optimization with SCF tolerance of 1.0×10^{-6} eV/atom under GGA-PBE potential [43].

A γ -Ni/ γ' -Ni₃Al interfacial supercell similar to that in literatures [12,27,32] is built, as shown in Fig. 1a. In which the (002) atomic layer is taken as a coherent interface of γ and γ' phases based on the experimental result reported by Harada et al. [49]. The lattice constant of the supercell is taken to be equal for γ -Ni and γ' -Ni₃Al blocks ($a\gamma \approx a\gamma' \approx 3.547$ Å) on the basis of the assumption of complete coherence. The interaction between two adjacent γ/γ' interfaces is neglected. Four sub-lattice sites and four octahedral interstitial centers are labeled by Arabic numerals (1, 2, 3, 4) and Roman numerals (i, ii, iii, iv), respectively. Each sub-lattice or octahedral interstice denotes a set of equivalent sites with same local environments at the γ/γ' interface. Since the (002) atomic layer can be regarded as either the surface of γ -blocks or the surface of γ' -blocks in present interfacial model, there exist two orientation relationships of (002) γ || (001) γ' and (001) γ || (002) γ' , as well as four constructional surface models, i.e., the (002) surface model of γ phases and the (001) surface model of γ' phases, and the (001) surface model of γ phases and the (002) surface model of γ' phases, respectively.

Previous experiments [50] and calculations [32] have revealed Re atoms to prefer to occupy Ni sub-lattice sites in γ phases and the substitution of Re for Ni at the coherent (002) γ/γ' interfacial layer is the most profitable for the strengthening of γ/γ' interfaces, hence, only a sort of Re-alloying interface, i.e., Re-2 model with the substitution of Re for Ni at the (002) γ/γ' layer, is selected to scale the strengthening effect of Re-addition in present investigation. Next, in order to examine the site preference of P at the γ/γ' interface, a series of γ -Ni/ γ' -Ni₃Al interfacial models with P-doping at various sub-lattice sites and octahedral interstitial centers are built. These doped systems are denominated as P–X models, where X (1, 2, 3, 4 or i, ii, iii, iv) represents sites doped by P. For consideration of symmetry, the γ/γ' interfacial supercell is doped by two P atoms, which are partitioned to two interfaces, and the symmetry of their distribution is maintained in subsequent calculations.

Finally, we constructed a set of the γ/γ' interfacial supercells with both P-doping and Re-addition, in which Re is fixed at the (002) γ/γ' atomic layer, similarly to Re-2 model, and then P is placed at octahedral interstitial centers or other Ni(Al) sub-lattice sites near by Re, as shown in Fig. 1b. The γ/γ' interface with duplex doping of P and Re is remarked as $M_{P-X}^{Re-2}(d)$, in which M represents the arrangement mode of Re and P (M = H means both of P and Re situate at the same atomic layer, M = V presents P locates at the adjacent atomic layers of Re); the superscript and subscript denote sites occupied by Re and P, respectively; d represents the correlative degree between P-doping and Re-addition. Herein, the d is differentiated by the initial distance d_{Re-P}^0 between P and Re, i.e., 1.774 Å, 2.508 Å, 3.547 Å and 4.344 Å, corresponding to P being doped at the first, the second, the third and the fourth nearest neighbors' sites of Re, respectively. For simplicity, the d is marked as 1st, 2nd, 3rd and 4th, respectively.

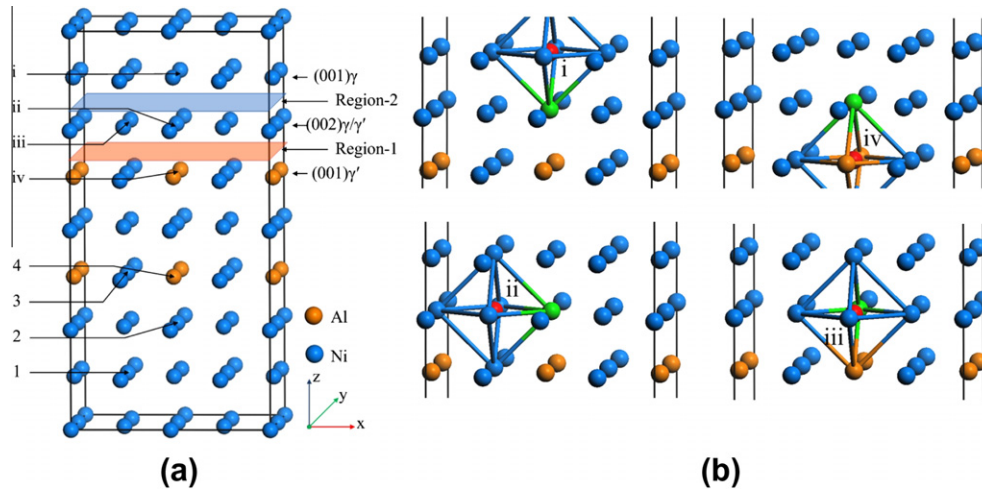


Fig. 1. The calculation model, (a) the γ -Ni/ γ' -Ni₃Al interfacial supercell, and (b) the typical interstitial octahedrons in the γ/γ' interfacial region. The blue, orange, green and red balls denote Ni, Al, Re and P atoms, respectively. (001) γ , (001) γ' and (002) γ/γ' present the (001) atomic layer in γ -Ni block, the (001) γ' atomic layer in γ' -Ni₃Al block and the γ/γ' interfacial atomic layer, respectively. Region-1 and Region-2 are the region bounded by the (002) γ/γ' and the (001) γ' layers and by the (001) γ and the (002) γ/γ' layers, respectively. The Arabic numerals 1, 2, 3, 4 and Roman numerals i, ii, iii, iv denote sub-lattice sites and octahedral interstitial centers in the γ/γ' interfacial supercell, respectively. (For interpretation of the references to color in this figure legend, the reader is referred to the web version of this article.)

3. Results and discussion

3.1. Site preference of P at the γ/γ' interface

In order to examine the probability of P-doping emerging at the γ -Ni/ γ' -Ni₃Al interface and to further determine its site preference in the interfacial region, herein the heat of formation H and the cohesive energy E of the γ -Ni/ γ' -Ni₃Al supercell are calculated by following expressions [51].

$$H = [E_i(n, m, l, k) - n \cdot E(\text{Ni}) - m \cdot E(\text{Al}) - l \cdot E(\text{P}) - k \cdot E(\text{Re})] / (m + n + l + k) \quad (1)$$

$$E = [E_i(n, m, l, k) - n \cdot E_{\text{Ni}} - m \cdot E_{\text{Al}} - l \cdot E_{\text{P}} - k \cdot E_{\text{Re}}] / (m + n + l + k) \quad (2)$$

where $E_i(n, m, l, k)$ is the total energy of the γ/γ' supercell with n , m , l and k atoms of Ni, Al, P and Re, respectively. $E(\text{Ni})$, $E(\text{Al})$, $E(\text{P})$ and $E(\text{Re})$ are the energies per atom in fcc-Ni, fcc-Al, triclinic-P and hcp-Re unit cells, respectively. E_{Ni} , E_{Al} , E_{P} and E_{Re} are the energies per gaseous Ni, Al, P and Re atoms, respectively. Table 2 tabulates the magnitude of H and E of the γ/γ' interface with or without P-doping. A negative H means P-doping at the γ/γ' interface is permissible from the energetic point of view. The larger the negative heat of formation is, the higher the formation ability of the doped γ/γ' interface is. In addition, the bigger the cohesive energy is, the more stable the doped system is [51]. Hence the following formation tendency of the Ni/Ni₃Al interface with or without P-doping can be deduced from the data presented in Table 2: P-1 > P-2 > P-3 > P-ii > P-i > P-4 > P-iii > P-iv > clean, in which clean model represents the interfacial supercell free of dopants. A larger negative H of the P-doped γ/γ' interface than the P-free γ/γ' interface suggests P can be doped in the γ/γ' interfacial region by occupying octahedral interstices or replacing a part of host atoms, similarly to S [27], B [12] and H as well as O and N [26]. In comparison with the octahedral interstices, P prefers to substitute for host atoms,

especially Ni atoms in γ -block. For P-doping at the coherent (002) γ/γ' layer, the favorable interstitial site is also octahedron ii bounded by 6 Ni atoms [27] rather than octahedron iii consisting of 5 Ni and a Al atom as proposed in Ref. [28], refer to Fig. 1b.

A comparison of the cohesive energy E exhibits the stability of the γ/γ' interface with or without P-doping declines in the following order: P-1 > P-4 > P-2 > P-3 > clean > P-ii > P-i > P-iii > P-iv. This means the γ/γ' interface with the substitution of P for host atoms is stable, while the γ/γ' interface with P-doping at the octahedral interstices is unstable relative to the γ/γ' interface free of P. A large cohesive energy E in P-1 model means the γ/γ' interface with P-doping at the (001) γ layer in γ -block is also the most stable. Therefore, P prefers to segregate to γ -Ni phases by occupying Ni1 sublattice sites, followed by Ni2 sites at the coherent (002) γ/γ' interfacial layer.

3.2. Effect of Re-addition on site preference of P at the γ/γ' interface

Similarly to the single P-doped interface, the heat of formation H and the cohesive energy E of the γ/γ' interface with both P-doping and Re-addition are also calculated. Table 3 lists the H and E values as well as the distance $d_{\text{Re-P}}$ between Re and P after cell optimization. It is observed that H values in the γ/γ' supercells with duplex doping of P and Re are also negative and their magnitudes are larger than those of single P-doped systems, which means P-doping either at the same atomic layer as Re or in adjacent atomic layers of Re is permissible in terms of energetics.

From Table 3, one can see that the magnitude of H and E is low as $d_{\text{Re-P}}$ being small, and the smaller the $d_{\text{Re-P}}$ is, the lower the magnitude of H and E is, which means P tends to keep away from Re in present duplex doping interfaces. As P being doped at an octahedral interstice near by Re, Table 3 shows the magnitude of H and E in $\text{H}_{\text{P-ii}}^{\text{Re-2}}(1^{\text{st}})$ and $\text{H}_{\text{P-iii}}^{\text{Re-2}}(1^{\text{st}})$ models is bigger than that in $\text{V}_{\text{P-i}}^{\text{Re-2}}(1^{\text{st}})$ and $\text{V}_{\text{P-iv}}^{\text{Re-2}}(1^{\text{st}})$ models, indicating P prefers to occupy octahedral interstices at the same (002) γ/γ' atomic layer as Re. For the

Table 2
The heat of formation H and the cohesive energy E of the γ/γ' interface with or without P.

Model	Clean	P-i	P-ii	P-iii	P-iv	P-1	P-2	P-3	P-4
H (V/atom)	-0.2627	-0.4186	-0.4235	-0.4003	-0.3398	-0.4743	-0.4684	-0.4453	-0.4112
E (eV/atom)	-5.6837	-5.6757	-5.6807	-5.6574	-5.5969	-5.7189	-5.713	-5.6899	-5.7150

Table 3

The heat of formation H and the cohesive energies E as well as the distances $d_{\text{Re-P}}$ between Re and P, at the γ/γ' interface with duplex doping of Re and P.

Model	$d_{\text{Re-P}}$ (Å)	H (eV/atom)	E (eV/atom)
$V_{\text{P-i}}^{\text{Re-2}}(1^{\text{st}})$	2.140	-0.3695	-5.8033
$V_{\text{P-1}}^{\text{Re-2}}(2^{\text{nd}})$	2.424	-0.4631	-5.8899
$V_{\text{P-1}}^{\text{Re-2}}(4^{\text{th}})$	4.334	-0.4666	-5.8934
$H_{\text{P-ii}}^{\text{Re-2}}(1^{\text{st}})$	2.235	-0.3979	-5.8318
$H_{\text{P-iii}}^{\text{Re-2}}(1^{\text{st}})$	2.239	-0.3799	-5.8137
$H_{\text{P-2}}^{\text{Re-2}}(2^{\text{nd}})$	2.497	-0.4539	-5.8808
$H_{\text{P-2}}^{\text{Re-2}}(3^{\text{rd}})$	3.626	-0.4567	-5.8835
$V_{\text{P-iv}}^{\text{Re-2}}(1^{\text{st}})$	2.185	-0.3418	-5.7756
$V_{\text{P-4}}^{\text{Re-2}}(2^{\text{nd}})$	2.636	-0.4054	-5.8914
$V_{\text{P-3}}^{\text{Re-2}}(2^{\text{nd}})$	2.533	-0.4324	-5.8592
$V_{\text{P-3}}^{\text{Re-2}}(4^{\text{th}})$	4.484	-0.4351	-5.8619

Table 4

The formation energies (E_{D}^{Re} , E_{D}^{P} and $E_{\text{D}}^{\text{Re-P}}$) of point defects and the correlative energy $\Delta E_{\text{D}}^{\text{Re-P}}$ between P-doping and Re-addition as well as the distance $d_{\text{Re-P}}$ between P and Re at the γ/γ' interface after cell optimization.

Model	$d_{\text{Re-P}}$ (Å)	E_{D}^{Re} (eV)	E_{D}^{P} (eV)	$E_{\text{D}}^{\text{Re-P}}$ (eV)	$\Delta E_{\text{D}}^{\text{Re-P}}$ (eV)
$V_{\text{P-i}}^{\text{Re-2}}(1^{\text{st}})$	2.140	5.8013	5.4183	9.6282	1.5914
$V_{\text{P-1}}^{\text{Re-2}}(2^{\text{nd}})$	2.424	5.8013	1.1242	6.5978	0.3277
$V_{\text{P-1}}^{\text{Re-2}}(4^{\text{th}})$	4.334	5.8013	1.1242	6.7091	0.2164
$H_{\text{P-ii}}^{\text{Re-2}}(1^{\text{st}})$	2.235	5.8013	5.5815	10.5692	0.8135
$H_{\text{P-iii}}^{\text{Re-2}}(1^{\text{st}})$	2.239	5.8013	4.8132	9.9713	0.6432
$H_{\text{P-2}}^{\text{Re-2}}(2^{\text{nd}})$	2.497	5.8013	0.9346	6.3041	0.4318
$H_{\text{P-2}}^{\text{Re-2}}(3^{\text{rd}})$	3.626	5.8013	0.9346	6.3917	0.3441
$V_{\text{P-iv}}^{\text{Re-2}}(1^{\text{st}})$	2.185	5.8013	2.8186	8.7156	-0.0957
$V_{\text{P-4}}^{\text{Re-2}}(2^{\text{nd}})$	2.636	5.8013	0.9992	6.6433	0.1572
$V_{\text{P-3}}^{\text{Re-2}}(2^{\text{nd}})$	2.533	5.8013	0.1953	5.6142	0.3824
$V_{\text{P-3}}^{\text{Re-2}}(4^{\text{th}})$	4.484	5.8013	0.1953	5.7012	0.2953

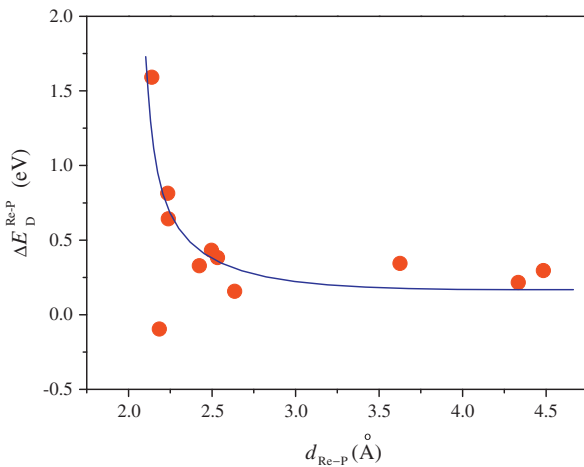


Fig. 2. The $d_{\text{Re-P}}$ dependence of the correlative energy $\Delta E_{\text{D}}^{\text{Re-P}}$ between P-doping and Re-addition at the γ/γ' interface.

substitution of P for host atoms at 2nd, 3rd or 4th nearest neighbors' sites of Re, the descending order of the magnitude of H and E : $V_{\text{P-1}}^{\text{Re-2}}(2^{\text{st}}) > H_{\text{P-2}}^{\text{Re-2}}(2^{\text{nd}}) > V_{\text{P-3}}^{\text{Re-2}}(2^{\text{nd}}) > V_{\text{P-4}}^{\text{Re-2}}(2^{\text{nd}})$ and $V_{\text{P-1}}^{\text{Re-2}}(4^{\text{th}}) > H_{\text{P-2}}^{\text{Re-2}}(3^{\text{rd}}) > V_{\text{P-3}}^{\text{Re-2}}(4^{\text{th}})$, reveals the most favorable substitution still takes place at the (001) γ layer in γ -Ni block, followed by the coherent (002) γ/γ' interfacial layer. This site preference is similar

Table 5

The Griffith rupture work W of the γ/γ' interface with or without dopants in different interfacial regions.

Site	Model	W (J/m ²)	Model	W (J/m ²)	Model	W (J/m ²)
Region-1	Clean	4.3864	Clean	4.3864	Clean	4.3864
Region-2		4.4319		4.4319		4.4319
Region-1	$V_{\text{P-i}}^{\text{Re-2}}(1^{\text{st}})$	4.4858	Re-2	4.4866	P-i	4.3145
Region-2		4.0043		4.9228		3.9005
Region-1	$V_{\text{P-1}}^{\text{Re-2}}(2^{\text{nd}})$	4.4604	Re-2	4.4866	P-1	4.3554
Region-2		4.6823		4.9228		4.2471
Region-1	$V_{\text{P-1}}^{\text{Re-2}}(4^{\text{th}})$	4.4803	Re-2	4.4866	P-1	4.3554
Region-2		4.6882		4.9228		4.2471
Region-1	$H_{\text{P-ii}}^{\text{Re-2}}(1^{\text{st}})$	3.9563	Re-2	4.4866	P-ii	3.8960
Region-2		4.2018		4.9228		3.9226
Region-1	$H_{\text{P-iii}}^{\text{Re-2}}(1^{\text{st}})$	3.8724	Re-2	4.4866	P-iii	3.7390
Region-2		4.2345		4.9228		3.9490
Region-1	$H_{\text{P-2}}^{\text{Re-2}}(2^{\text{nd}})$	4.1147	Re-2	4.4866	P-2	4.0445
Region-2		4.6098		4.9228		4.2752
Region-1	$H_{\text{P-2}}^{\text{Re-2}}(3^{\text{rd}})$	4.1139	Re-2	4.4866	P-2	4.0445
Region-2		4.7531		4.9228		4.2752
Region-1	$V_{\text{P-iv}}^{\text{Re-2}}(1^{\text{st}})$	4.0799	Re-2	4.4866	P-iv	3.9566
Region-2		4.9606		4.9228		4.4358
Region-1	$V_{\text{P-4}}^{\text{Re-2}}(2^{\text{nd}})$	4.3993	Re-2	4.4866	P-4	4.3798
Region-2		4.9319		4.9228		4.4455
Region-1	$V_{\text{P-3}}^{\text{Re-2}}(2^{\text{nd}})$	4.5752	Re-2	4.4866	P-3	4.5742
Region-2		4.7762		4.9228		4.3063
Region-1	$V_{\text{P-3}}^{\text{Re-2}}(4^{\text{th}})$	4.6222	Re-2	4.4866	P-3	4.5742
Region-2		4.8451		4.9228		4.3063

to that in the single P-doped system. No evident influence of local environments on the site preference of P is detected in present duplex doping interfacial system. This is said, the site preference of P at the γ/γ' interface is not changed by Re-addition. In comparison with the single P-doped interfaces, although the formation ability of the duplex doping system is slightly low, their structural stability is obviously elevated, specifically in the substitution of P for Ni1 near by Re.

3.3. Interaction between P-doping and Re-addition at the γ/γ' interface

As mentioned above, P is permissible to be doped at the Re-alloyed γ/γ' interface by means of substitutional or interstitial solid solution mode. Owing to the content of P and Re being very low in the Ni-based SC superalloys, P-doping and Re-addition at the γ/γ' interface can be regarded as point defects. Thereby, the interaction between P-doping and Re-addition, i.e., the correlative energy $\Delta E_{\text{D}}^{\text{Re-P}}$ between point defects, can be calculated by following expressions [52]:

$$\Delta E_{\text{D}}^{\text{Re-P}} = E_{\text{D}}^{\text{Re-P}} - (E_{\text{D}}^{\text{Re}} + E_{\text{D}}^{\text{P}}) \quad (3)$$

$$E_{\text{D}}^{\text{X}} = E_{\text{i}}^{\text{X}}(m-x, n-y, l, k) - E_{\text{i}}^{\text{clean}}(m, n, 0, 0) - l \cdot E(\text{P}) - k \cdot E(\text{Re}) + x \cdot E(\text{Ni}) + y \cdot E(\text{Al}) \quad (4)$$

where $X = \text{Re}, \text{P}$ and P-Re . E_{D}^{X} is the formation energy of the X point defects. $E_{\text{i}}^{\text{X}}(m-x, n-y, l, k)$ and $E_{\text{i}}^{\text{clean}}(m, n, 0, 0)$ are the total energies of the interfacial supercell with and without X defect, respectively. x and y denote the numbers of Ni and Al atoms replaced by dopants in the interfacial supercell, respectively. The calculated $\Delta E_{\text{D}}^{\text{Re-P}}$ is given in Table 4.

From Table 4, one can see that the $\Delta E_{\text{D}}^{\text{Re-P}}$ values are positive in all duplex doping systems except $V_{\text{P-i}}^{\text{Re-2}}(1^{\text{st}})$ (d) model, meaning a strong repulsive interaction to exist between P-doping and Re-addition [52]. And the magnitude of $\Delta E_{\text{D}}^{\text{Re-P}}$ decreases in the following order: $V_{\text{P-i}}^{\text{Re-2}}(1^{\text{st}}) > H_{\text{P-iii}}^{\text{Re-2}}(1^{\text{st}}) > H_{\text{P-2}}^{\text{Re-2}}(2^{\text{nd}}) > V_{\text{P-2}}^{\text{Re-2}}(2^{\text{nd}}) >$

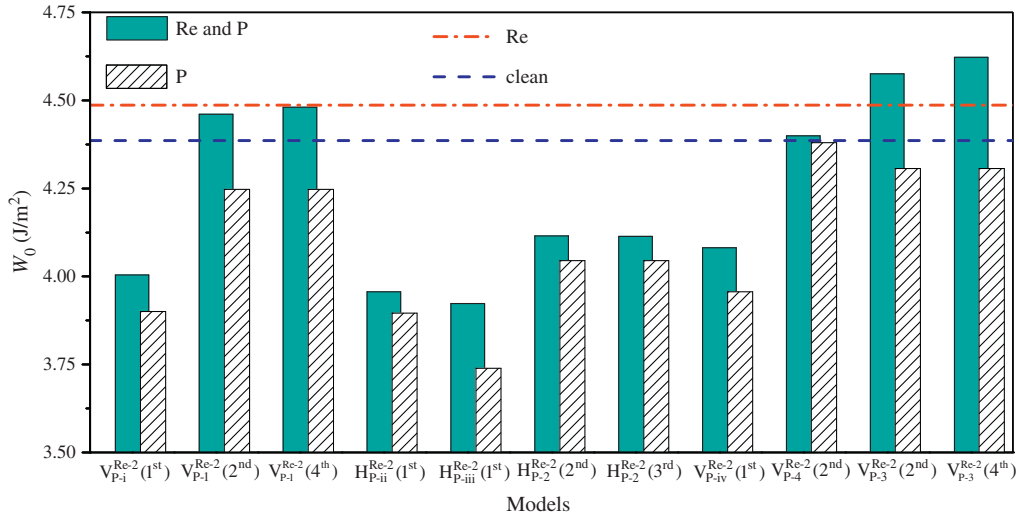


Fig. 3. The inter-phase fracture strength W_0 of the γ/γ' interface with or without dopants.

$V_{P-3}^{Re-2} (2^{nd}) > H_{P-2}^{Re-2} (3^{rd}) > V_{P-1}^{Re-2} (4^{th}) > V_{P-3}^{Re-2} (4^{th}) > V_{P-1}^{Re-2} (4^{th}) > V_{P-4}^{Re-2} (2^{nd})$. This tendency seems to imply an increasing distance d_{Re-P} between P and Re leads to the correlative interaction between P-doping and Re-addition to reduce. Fig. 2 further illustrates the d_{Re-P} dependence of correlation energies ΔE_D^{Re-P} , which clearly shows the magnitude of ΔE_D^{Re-P} increases with decreasing d_{Re-P} as P being doped either at the adjacent atomic layers of Re or at the same atomic layer as Re. With the ascent of d_{Re-P} from 2.20 Å to 2.75 Å, the magnitude of ΔE_D^{Re-P} descends sharply, followed by a slowly drop, and then tends to constant (about 0.2 eV) as $d_{Re-P} \geq 3.00$ Å. It is noted that a strong correlation between P-doping and Re-addition is limited in the range of 2.75 Å. Beyond the limit, the interaction between P-doping and Re-addition is weak and independent on d_{Re-P} . This limited d_{Re-P} is approximately equal to the distance ($d \approx 2.508$ Å) between first near neighbor's sites at the γ/γ' interface but smaller than the crystal constant ($a_\gamma \approx a_{\gamma'} \approx 3.547$ Å) of γ -Ni or γ' -Ni₃Al phase, which means the strong correlation between P-doping and Re-addition exists in only an unit cell for present duplex doping γ/γ' system. Since the correlation energy ΔE_D^{Re-P} can characterize the correlative degree of P-doping and Re-addition to some extent, in the following sections the ΔE_D^{Re-P} will replace d_{Re-P} to evaluate the correlative and synergistic effect of P and Re on fracture properties of the γ/γ' interface.

3.4. Griffith rupture work of the γ/γ' interface with duplex doping of P and Re

It is widely acceptable that the γ/γ' interface is the weakest region in Ni-based SC superalloys. The binding strength of the γ/γ' interface can be regarded as a representative of the rupture strength of Ni-based SC superalloys to a certain degree [32]. The work of separation, i.e., the Griffith rupture work W [10], which is defined as the reversible work needed to separate a crystal along the interface into two free surfaces, is employed to evaluate the binding strength of the γ/γ' interface. W can be calculated by means of a difference in the total energy between the optimized interfacial model and the corresponding surface models:

$$W = (-1/2S_i) \cdot [E_i(n, m, l, k) - E_S^\gamma(n_\gamma, m_\gamma, l_\gamma, k_\gamma) - E_S^{\gamma'}(n_{\gamma'}, m_{\gamma'}, l_{\gamma'}, k_{\gamma'})] \quad (5)$$

where S_i is the area of the coherent atomic layer in the γ/γ' interfacial model. $E_S^\gamma(n_\gamma, m_\gamma, l_\gamma, k_\gamma)$ and $E_S^{\gamma'}(n_{\gamma'}, m_{\gamma'}, l_{\gamma'}, k_{\gamma'})$ are the total

energies of γ and γ' surface models, respectively, corresponding to the γ/γ' interfacial model. n, m, l, k denote the numbers of Ni, Al, P and Re atoms, respectively, where $n = n_\gamma + n_{\gamma'}$, $m = m_\gamma + m_{\gamma'}$, $l = l_\gamma + l_{\gamma'}$, $k = k_\gamma + k_{\gamma'}$. Herein, the surface models truncated from the

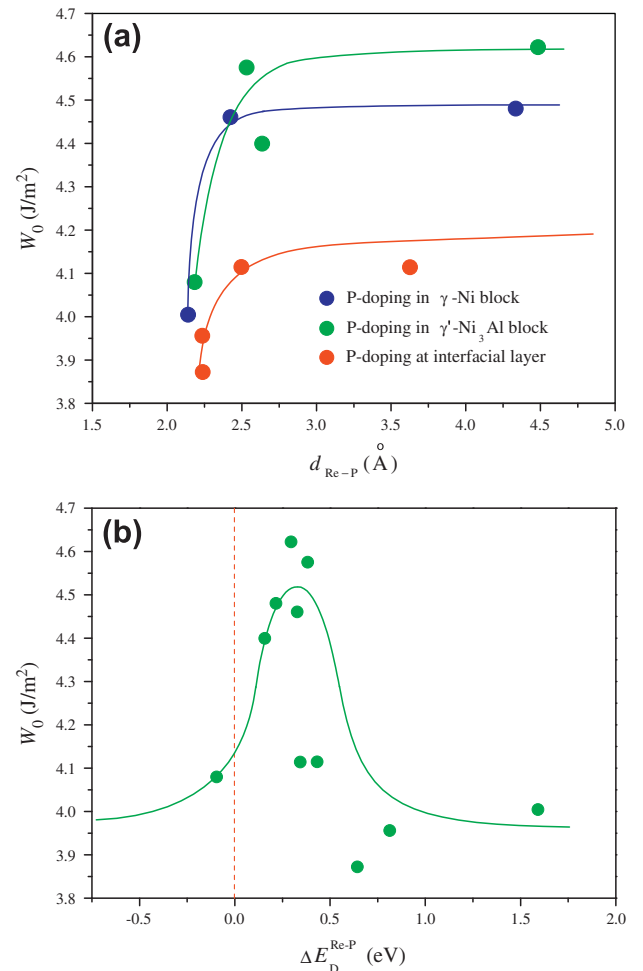


Fig. 4. The inter-phase fracture strength W_0 of the γ/γ' interface as functions of (a) d_{Re-P} and (b) ΔE_D^{Re-P} .

optimized interfacial supercells will not be relaxed in the calculation of the cleavage work W .

Table 5 tabulates the Griffith rupture works W of the γ/γ' interface with duplex doping of P and Re and corresponding clean and P-doped systems calculated by using Eq. (5). Since there are two orientation relationships, i.e., $(002)\gamma\parallel(001)\gamma'$ and $(001)\gamma\parallel(002)\gamma'$ in present γ/γ' interfacial model, there are two potential inter-phase fracture sites [12,27,32], i.e., region-1 and region-2 as illustrated in Fig. 1. In the mode related to $(002)\gamma\parallel(001)\gamma'$, the cleavage adjacent to the coherent $(002)\gamma/\gamma'$ atomic layer occurs along the $(001)\gamma'$ layer of γ' blocks, while in the mode related to $(001)\gamma\parallel(002)\gamma'$, the split takes place along the $(001)\gamma$ layer of γ blocks.

It is noted that the Griffith rupture work W in Region-1 is smaller than that in region-2 at the clean γ/γ' interface. Since the fracture usually emerges at the weakest part of a material [10], the Griffith rupture work W in region-1, 4.3864 J/m², represents the rupture strength W_0 of the clean γ/γ' interface [12,32]. In the case of single Re-addition at the $(002)\gamma/\gamma'$ layer, the Griffith rupture work W in region-1 is also smaller than that in region-2, but increases by 2.3% relative to the clean γ/γ' interface [32], which means Re-addition can strengthen the γ/γ' interface as reported in literatures [2–4]. However, Table 5 shows the Griffith rupture work W of the single P-doped γ/γ' interface is generally smaller than that of the clean γ/γ' interface even though the inter-phase fracture site is changed to region-2 in some P-doping systems, e.g., P-i, P-1 and

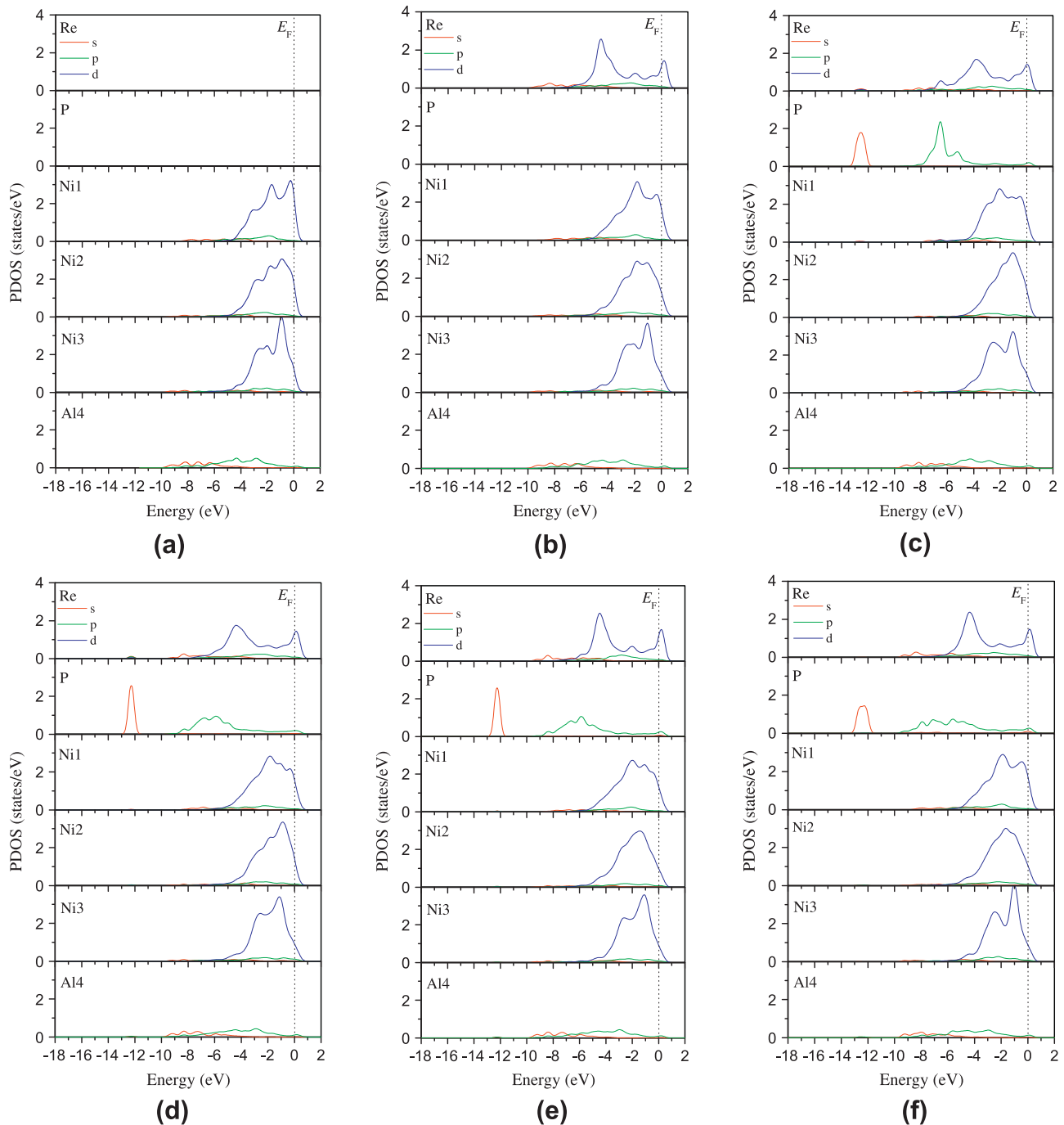


Fig. 5. The partial densities of states PDOS of host and doping atoms in (a) clean, (b) Re-2, (c) $V_{P,i}^{Re-2}$ (1st), (d) $H_{P,2}^{Re-2}$ (2nd), (e) $H_{P,2}^{Re-2}$ (3rd) and (f) $V_{P,3}^{Re-2}$ (4th) supercells.

P-3 models. This notable weakening influence indicates P is indeed a deleterious dopant for the rupture strength of the γ/γ' interface of Ni-based SC superalloys [11]. With respect to the γ/γ' interface with both P-doping and Re-addition, the Griffith rupture works W in region-1 are smaller than those in region-2 except for V_{P-i}^{Re-2} (1st) model, which means an extra P-doping does not change the cleavage fracture site at the Re-alloyed γ/γ' interface. The cleavage of γ/γ' interfaces with duplex doping of Re and P still takes place in region-1, i.e., the region between the (002) γ/γ' layer and the (001) γ' layer.

Fig. 3 further illustrates the rupture strengths W_0 of γ/γ' interfaces with or without dopants. A comparison of the Griffith rupture work reveals the inter-phase rupture strength W_0 of the γ/γ' interface with duplex doping of P and Re is generally higher than that of corresponding single P-doped system, but lower than that of the single Re-alloyed interface. In V_{P-3}^{Re-2} (2nd) and V_{P-3}^{Re-2} (5th) models, the rupture strength W_0 even increases by 0.0886 J/m² and 0.1356 J/m², respectively, compared with the single Re-alloyed system. Obviously, Re can inhibit P-induced embrittlement at the γ/γ' interface, similarly to the influence of Re on the S-doped interface [28]. Relative to the clean γ/γ' interface, the rupture strengths W_0 are low in H_{P-ii}^{Re-2} (1st), H_{P-iii}^{Re-2} (1st), H_{P-2}^{Re-2} (2nd) and H_{P-2}^{Re-2} (3rd) models but high in V_{P-i}^{Re-2} (2nd), V_{P-1}^{Re-2} (4th), V_{P-4}^{Re-2} (2nd), V_{P-3}^{Re-2} (2nd) and V_{P-3}^{Re-2} (4th)

models. This result seems to imply the synergetic effect of P and Re along the interfacial atomic layer is different from that across the interfacial atomic layer at present duplex doping system.

In order to examine the influence of interaction between Re and P on the inter-phase rupture strength W_0 of the γ/γ' interface, Fig. 4a plots the d_{Re-P} dependence of the rupture strengths W_0 at the γ/γ' interface with duplex doping of Re and P. A similar variation tendency to ΔE_D^{Re-P} vs d_{Re-P} as described in Section 3.3 can be seen. That is, either for P-doping at the adjacent atomic layer of Re, i.e., the (00) γ layer in γ -block and the (001) γ' layer in γ' -block, or for P-doping at the same atomic layer as Re, i.e., the (002) γ/γ' interfacial layer, the inter-phase rupture strength W_0 ascends rapidly with increasing d_{Re-P} before $d_{Re-P} \leq 2.75$ Å, and then tends toward constant after $d_{Re-P} \geq 3.00$ Å. It is noted that the site of P at the Re-alloyed interface indeed plays an important role on the interfacial rupture strength W_0 . Relative to P-doping at the same atomic layer as Re, P-doping at the adjacent atomic layer of Re, specifically at the (001) γ' atomic layer in γ' -block, is less harmful for the Re-enforced γ/γ' interface.

Fig. 4b further illustrates the relation of the rupture strength W_0 with the correlative energy ΔE_D^{Re-P} . From Fig. 4b, one can see that the W_0 value of the γ/γ' interface with duplex doping of Re and P rapidly ascends in the range of -0.5 eV to 0.3 eV, and then falls down sharply with increasing ΔE_D^{Re-P} , finally tends to constant as

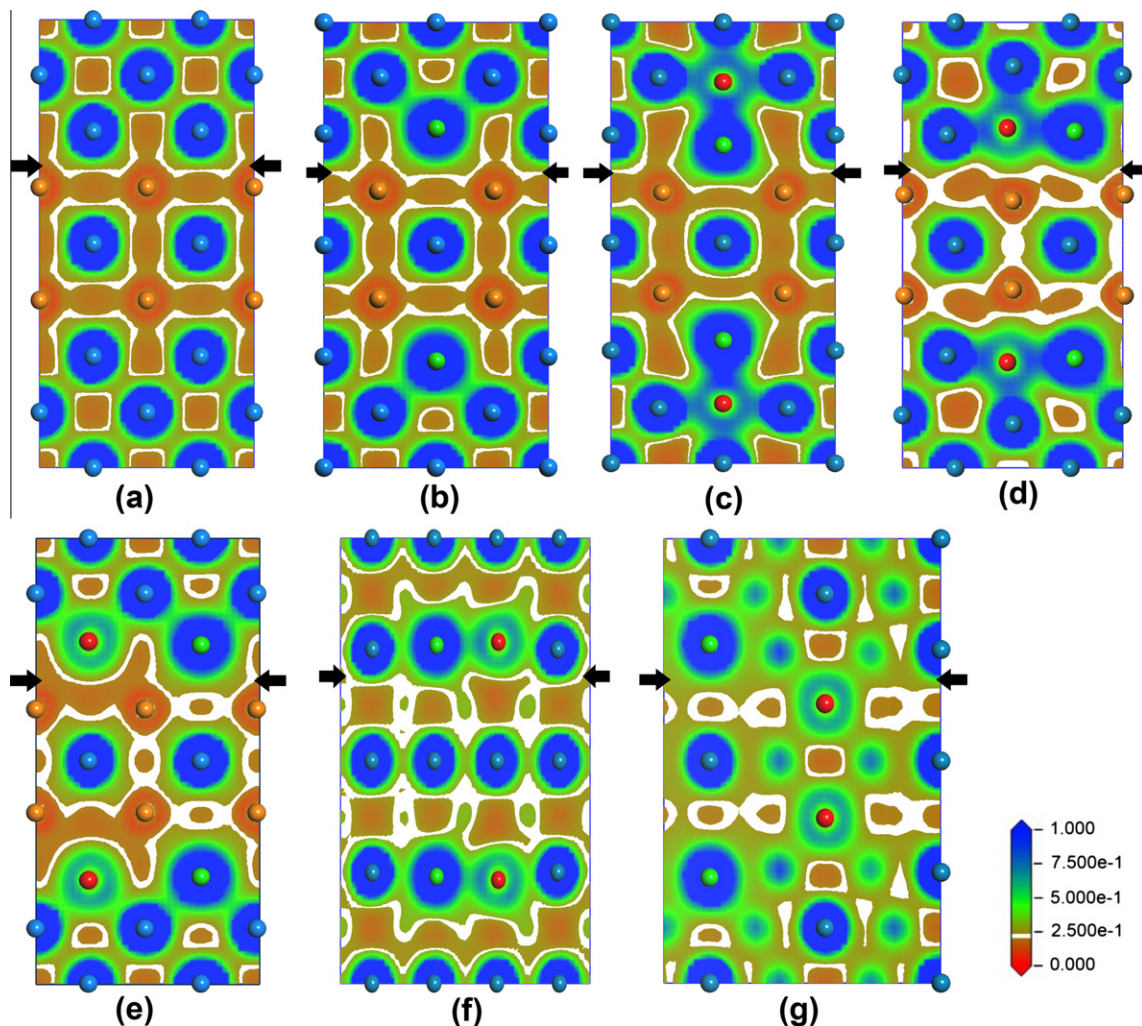


Fig. 6. The total valence charge density contour plots on sections across the interface in the γ -Ni/ γ' -Ni₃Al interfacial model with or without dopants. (a) (200) plane in clean model, (b) (200) plane in Re-2 model, (c) (200) plane in V_{P-i}^{Re-2} (1st) model, (d) (200) plane in H_{P-iii}^{Re-2} (1st) model, (e) (200) plane in H_{P-2}^{Re-2} (3rd) model, (f) (110) plane in H_{P-2}^{Re-2} (2nd) model and (g) (420) plane in V_{P-3}^{Re-2} (4th) model. The blue, orange, green and red balls denote Ni, Al, Re and P atoms, respectively. The region indicated by solid arrows is the inter-phase fracture site. (For interpretation of the references to color in this figure legend, the reader is referred to the web version of this article.)

Table 6

Space between atomic layers in γ -Ni block, γ -Ni₃Al block, Region-1 and Region-2 in the γ -Ni/ γ -Ni₃Al interfacial models with or without dopants (unit: Å).

Model	Ni-block	Region-2	Region-1	Ni ₃ Al-block
Clean	1.783	1.770	1.795	1.798
Re-2	1.792	1.798	1.803	1.826
V _{P-i} ^{Re-2} (1 st)	1.899	1.889	1.826	1.861
V _{P-i} ^{Re-2} (2 nd)	1.781	1.800	1.812	1.799
V _{P-i} ^{Re-2} (4 th)	1.776	1.786	1.788	1.815
H _{P-ii} ^{Re-2} (1 st)	1.795	1.838	1.896	1.751
H _{P-iii} ^{Re-2} (1 st)	1.812	1.841	1.854	1.808
H _{P-2} ^{Re-2} (2 nd)	1.815	1.822	1.839	1.805
H _{P-2} ^{Re-2} (3 rd)	1.815	1.821	1.787	1.843
V _{P-iv} ^{Re-2} (1 st)	1.756	1.805	1.863	1.865
V _{P-4} ^{Re-2} (2 nd)	1.793	1.772	1.810	1.790
V _{P-3} ^{Re-2} (2 nd)	1.741	1.737	1.774	1.735
V _{P-3} ^{Re-2} (4 th)	1.736	1.765	1.779	1.726

$\Delta E_D^{\text{Re-P}} \geq 1.0$ eV. Obviously, a big W_0 value emerges in the range of $0.2 \text{ eV} \geq \Delta E_D^{\text{Re-P}} \geq 0.5$ eV. That means both strong repulsive and weak attractive interaction between Re-addition and P-doping are not advantageous for the strengthening of the γ/γ' interface. As elaborated in Section 3.3, the strong correlation between P-doping and Re-addition is limited in the range of 2.75 Å. Beyond the limit, the correlation between P-doping and Re-addition becomes a weak repulsive interaction of about 0.2 eV. Hence, the detrimental effect of P on the Re-alloyed γ/γ' interface can be attributed to a strong repulsive interaction between P-doping and Re-addition to some extent.

3.5. Electronic structure and local elastic strain energy of the γ/γ' interface

The partial densities of states (PDOS) of Re, P, Ni1, Ni2, Ni3 and Al4 atoms in the γ/γ' interfacial model with or without dopants are plotted in Fig. 5 to deeply understand the bonding characteristics

of the γ/γ' interface. Fig. 5a shows the bonding between FNN Ni–Ni atoms in γ -Ni block is mainly metallic bonding due to numerous Ni-3d valence electrons $N(E_F)$ at Fermi energy level E_F . In the γ' -Ni₃Al block, few Al-3p valence electrons at E_F and a broad overlap between Ni-3d/4p and Al-3p valence electrons below E_F indicate only a covalent bonding to exist between FNN Ni–Al atoms. That means for the clean interfacial system the binding strength between γ -block and γ' -block in region-2 is mainly dominated by metallic bonding between FNN Ni1–Ni2 atoms, whereas an influence of covalent bonding between FNN Ni2–Al4 atoms cannot be ignored in region-1 besides metallic bonding between FNN Ni2–Ni3 atoms [28,32].

With the addition of Re, the PDOS curves in Fig. 5b reveals the majority of metallic bonding in region-2 and a sum of metallic bonding and covalent bonding in region-1 is not affected by Re-addition. The bonding electrons of Re mainly results from Re-5d shell, and rich Re-6s/6p valence electrons make the covalent bonding between Re and its FNN atoms distinctly increase relative to the Re-free interface [32]. Hence, the strengthening effect of Re on the γ/γ' interface primarily originates from the enhanced Re–Ni and Re–Al interactions, similarly to the influence of Re on the tensile and shear strength of γ' -Ni₃Al phase [34].

In the P-doped interfacial system, Fig. 5c shows the interaction between P and its FNN atoms is mainly covalent bonding, in which the interaction between P-3p and Al-3s/3p is the strongest and the bonding between P-3p and Ni-3d is weaker than that between P-3p and Re-5d. In addition, some valence electrons of P atom transfer to its FNN Ni and Re atoms, leading to the emergence of a new bonding peak at the level of -13 eV to -12 eV. That means the interaction between FNN P–Ni or P–Re atoms is a complex of ionic bonding and covalent bonding. However, from Fig. 5e and f, it is noticed this extra covalent bonding between P-3s and Re-5d/6s/6p only exists in the case of P being doped at 1st or 2nd near neighbors' site of Re.

Fig. 6 further illustrates several typical total valence electron density contour plots on the cross section of the two coherent

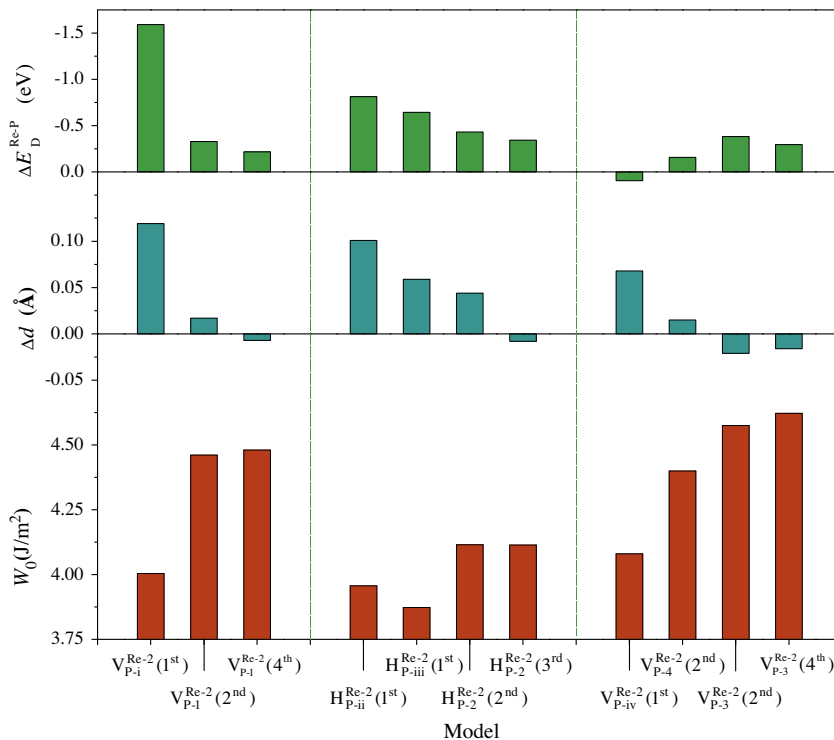


Fig. 7. The correlation of the inter-phase fracture strength W_0 at the doped γ/γ' interface with the difference of separation of region-1 between the doped and clean systems Δd as well as the correlative energy between P-doping and Re-addition $\Delta E_D^{\text{Re-P}}$.

interfacial layers of the γ/γ' interface with or without dopants. At the clean γ/γ' interface, the interaction between FNN Ni–Al atoms in γ' block is stronger than that between FNN Ni–Ni atoms in γ block [53]. Moreover, a significant anisotropic build-up of the directional d bonding charge of Ni atoms in γ' block, which is caused mainly by the polarization of Al- p electrons as a result of the p - d hybridization effect, along FNN Ni–Al direction [53], can be also observed. For the Ni atoms in γ block, which is far from Al in γ' block, the interaction between FNN Ni–Ni atoms displays an obvious isotropy. On the whole, the valence charge density plot on the (200) plane at the clean γ/γ' interface illustrates that the valence charge density in region-2 is rich but poor in region-1. This means the local electronic interaction in region-2 is stronger than that in region-1, a potential inter-phase cleavage fracture at the clean γ/γ' interface will therefore take place in region-1 between the (001) γ' and (002) γ/γ' layers [12,29,32]. Thus, the total valence charge density contour plots at the clean interface provide a direct visual pattern for understanding the inter-phase rupture sites indicated in Table 5.

In the case of substitution of Re for Ni at the (002) γ/γ' layer, the contour plots of valence charge density are similar to those of the clean interface in terms of the fracture site at the γ/γ' interface. And, the increasing W_0 in Re-2 model should be derived from a more enrichment of electron densities between FNN Ni1–Re in γ -Ni block compared with those of the clean system.

With respect to the doped system, Fig. 6c and d shows the extra doping causes an evident displacement of host atoms near by P. All host and Re atoms adjacent to P are found to be pushed away from their sub-lattice sites. And the longitudinal displacement, i.e., across the γ/γ' interface, of Ni, Al or Re atom at the upper and lower vertexes of the occupied octahedron is more than the horizontal displacement, i.e., along the γ/γ' interface, of host and alloyed atoms at the P-doped atomic layer. In addition, the doping atom is also found to displace toward the same direction as the above activated Ni, Al or Re in these P-doped systems. This indicates the deformation of the interstitial P-doped γ/γ' interface is the displacement of the whole distorted octahedron to some extent. Undoubtedly, this whole displacement of distorted octahedrons consequentially causes the space between atomic layers to be changed, especially for region-1 and region-2, similarly to S-doped systems [27]. Thus, on the one hand, with the displacement of the doping atom and its adjacent host and alloyed atoms, the electron densities at the interfacial region will be redistributed; on the other hand, the variation of interfacial separations will also yield extra local elastic strain energy at the cohesive site between γ -block and γ' -block [25].

In $V_{p-i}^{Re-2}(1^{st})$ and $H_{p-iii}^{Re-2}(1^{st})$ models, the enrichment of valence electrons along P–Ni1, P–Ni2 and P–Re means strong covalent bonding between P and its FNN Ni as well as Re to lie in γ -Ni block. These strong electronic interactions further make the (002) γ/γ' interfacial layer and γ -Ni phase become one whole block, therefore, the inter-phase fracture takes place in region-1 between the (002) γ/γ' and (001) γ' layers, as showed in Table 5. In the case of P being doped at the 2nd near neighbors of Re, a strong P–Re bonding can also be observed, although the repulsive interaction between P and Re exists still in $H_{p-2}^{Re-2}(2^{nd})$ model. From Fig. 6f, one can see that the depletion of valence electron densities in region-1 and the enrichment in region-2 are not affected by P-doping, but P-doping causes the electron densities in region-1 to be further depleted, hence its rupture strength W_0 listed in Table 5 is lower than that at the clean interface. As P being far away from Re, Fig. 6e and g shows the electronic interaction between Re and P becomes very weak, but the distribution of valence electrons is still depletive in region-1 and enriched in region-2. Therefore the preferential emergence of cleavage fracture in region-1 can also be understand in $H_{p-2}^{Re-2}(3^{rd})$ and $V_{p-3}^{Re-2}(4^{th})$ models.

However, it is noticed that the space between the (002) γ/γ' and (001) γ' layers in $H_{p-2}^{Re-2}(3^{rd})$ model is significantly bigger than that in $V_{p-3}^{Re-2}(4^{th})$ model. As well-known, for P-induced embrittlement at the γ/γ' interface, one of the reasons is the large atomic size of P atoms [54], which push host atoms away from their initial positions and lead to a variation of interfacial structures. In contrast, Re is called as an enhancer because it can resist the deformation of the γ/γ' interface due to a strong metallic bonding between Re and host atoms [34]. As P and Re being simultaneously doped at the γ/γ' interface, the strong repulsive interaction between Re-addition and P-doping will inevitably affect the local environment around doping atoms and then cause a large lattice distortion in the interfacial region. As a result of the lattice distortion, a extra local elastic strain energy [25,27] will be introduced at doped interfacial systems.

In order to evaluate the influence of local elastic strain energy on the binding strength of doped γ/γ' interfaces, the space between atomic layers is further examined after cell optimization. Table 6 tabulates the space between atomic layers in γ -Ni block, γ' -Ni₃Al block, Region-1 and Region-2 in the γ/γ' interfacial supercells with or without dopants. From Table 6, one can see that the separation of region-1 is obviously bigger than that of region-2 in all doped systems except for $V_{p-i}^{Re-2}(1^{st})$ model. A large separation and less electron densities means the cohesive strength of region-1 is weak compared with region-2, therefore the inter-phase cleavage fracture occurs in region-1 at most of the doped systems. In this case, a particular attention will be paid to the variation of separation of region-1 caused by P-doping, and then the difference Δd of separation of region-1 between the doped and clean interfaces is calculated further by the following expression:

$$\Delta d = d_{\text{region-1}}^{\text{doping}} - d_{\text{region-1}}^{\text{clean}} \quad (6)$$

where $d_{\text{region-1}}^{\text{doping}}$ and $d_{\text{region-1}}^{\text{clean}}$ are separations of region-1 at the γ/γ' interfaces with and without doping, respectively. Fig. 7 illustrates the Δd values at doped γ/γ' interfaces. For the convenience of comparison, the rupture strengths W_0 and the correlative energies between P-doping and Re-addition ΔE_D^{Re-P} in these doped systems are also represented in Fig. 7. For P-doping at 1st and 2nd near neighbors' sites of Re, the Δd value is found to be positive and big, whereas it is negative and small in the case of P being doped at 3rd and 4th near neighbors' sites of Re. A positive Δd means the interfacial separation is extended. On the contrary, a negative Δd indicates a shrinkage takes place in the cohesive region between γ -block and γ' -block. With the enlargement of separation, the local elastic strain energy increases. However, in the shrunk case, the electronic interaction in the interfacial region, i.e., atomic bonding energy, is also improved due to shortened bonding strengths [27]. That is said, the rupture strength of the doped γ/γ' interface will depend on a mutual influence of local elastic strain energy and atomic bonding energy in the interfacial region.

In the case of P near by Re, a strong correlation and repulsive interaction between P-doping and Re-addition brings about a significant enlargement of interfacial separation. Therefore, low rupture strengths in $V_{p-i}^{Re-2}(1^{st})$, $V_{p-iv}^{Re-2}(1^{st})$, $H_{p-iii}^{Re-2}(1^{st})$ and $H_{p-ii}^{Re-2}(1^{st})$ models can be attributed to their excessive local elastic strain energies in the inter-phase fracture region-1. As P being far away from Re, Table 3 shows the correlation degree between P-doping and Re-addition is very weak, but a synergetic effect of P and Re on the space between atomic layers can be still seen from Fig. 6. In $V_{p-3}^{Re-2}(2^{nd})$ and $V_{p-3}^{Re-2}(4^{th})$ models, both P and Re doped at the upper and lower sides of region-1 make the interfacial separation shrunken due to strong P–Ni(Al) covalent bonding and Re–Ni(Al) metallic bonding. Undoubtedly, this shrunken separation caused by the synergetic effect of P and Re can improve the bonding strength between γ -block and γ' -block, thereby, it should be

responsible for their high rupture strengths W_0 in V_{P-3}^{Re-2} (2^{nd}) and V_{P-3}^{Re-2} (4^{th}) models.

4. Conclusion

Using the first-principles plane-wave pseudo potential method, a systematic investigation of the synergetic effect of Re and P on the rupture strength of the γ/γ' interface has been performed. The calculated results of the heat of formation and the cohesive energy indicate Re and P can coexist in the γ/γ' interfacial region, and the site preference of P at the γ/γ' interface is not changed by Re-addition. In the duplex doping system, a synergetic effect of Re and P on the rupture strength of the γ/γ' interface has been found. As P being close to Re, the rupture strength of the doped interface is lower than that in the case of P apart from Re, and the rupture strength of the γ/γ' interface with P-doping at the adjacent atomic layer of Re, i.e., the (001) γ or (001) γ' atomic layer, is high compared with the interface doped by P at the same (002) γ/γ' atomic layer as Re. A correlative energy ΔE_D^{Re-P} between P-doping and Re-addition is adopted to characterize the mutual influence of P and Re at the doped γ/γ' interface. Results show a strong correlation and repulsive interaction between P-doping and Re-addition is limited in the range of $d_{Re-P} \leq 2.75 \text{ \AA}$, and the strong repulsive interaction between Re-addition and P-doping is not advantageous for the strengthening of the γ/γ' interface. A further analysis of electronic structures and local elastic strain energies reveals both P–Ni(Al) covalent bonding and Re–Ni metallic bonding are stronger than the electronic interactions between corresponding host atoms in the clean interface. The strengthening effect of Re on the γ/γ' interface mainly arises from the enhanced Re–Ni and Re–Al interactions. A large separation and the depletion of electron densities in region-1 should be responsible for the potential inter-phase fracture site at the doped system, and the P-induced embrittlement can be attributed to a mutual influence of local elastic strain energy and atomic bonding energy in the Re-alloyed γ/γ' system. With the close of P to Re, the excessive local elastic strain energies originated from the strong correlative interaction between Re-addition and P-doping plays an important role in weakening the binding strength between γ -phase and γ' -phase. As P being doped on the other sides of Re across interfacial layer, however, the rupture strength of the Re-alloyed γ/γ' interface can even profit from the shrunken separation caused by the synergetic effect of P and Re.

Acknowledgments

Financial support of the present research from the National Natural Science Foundation of China (50771044 and 51071065) and from the Major State Basic Research Development Program of China (2010CB631206) is gratefully acknowledged.

References

- [1] Y. Yamabe-Mitarai, Y. Ro, T. Maruko, H. Harada, *Metall. Mater. Trans. A* 29 (1998) 537–549.
- [2] J.J. Yu, X.F. Sun, T. Jin, N.R. Zhao, H.R. Guan, Z.Q. Hu, *Mater. Sci. Eng. A* 458 (2007) 39–43.
- [3] C.M.F. Rae, R.C. Reed, *Acta. Mater.* 49 (2001) 4113–4325.
- [4] P. Caron, T. Khan, *Aerosp. Sci. Technol.* 3 (1999) 513–523.
- [5] R.A. Hobbs, L. Zhang, C.M.F. Rae, S. Tin, *Metall. Trans. A* 39 (2008) 1014–1025.
- [6] K. Harris, J.B. Wahl, *Mater. Sci. Technol.* 25 (2009) 147–153.
- [7] L.X. Yu, Y.R. Sun, W.R. Sun, X.F. Sun, S.R. Guo, Z.Q. Hu, *Mater. Sci. Eng. A* 527 (2010) 911–916.
- [8] Z.Q. Hu, W.R. Sun, S.L. Yang, S.R. Guo, H.C. Yang, *Mater. Trans.* 50 (2009) 1638–1643.
- [9] Y.F. Gu, Y. Yamabe-Mitarai, T. Yokokawa, H. Harada, *Mater. Lett.* 57 (2003) 1171–1178.
- [10] Q.M. Hu, R. Yang, D.S. Xu, Y.L. Hao, D. Li, W.T. Wu, *Phys. Rev. B* 67 (2003) 224203.
- [11] J.W. Cohron, E.P. George, L. Heatherly, C.T. Liu, R.H. Zee, *Acta. Mater.* 45 (1997) 2801–2811.
- [12] P. Peng, D.W. Zhou, J.S. Liu, R. Yang, Z.Q. Hu, *Mater. Sci. Eng. A* 416 (2006) 169–175.
- [13] A.P. Ofori, C.J. Rossouw, C.J. Humphreys, *Acta. Mater.* 53 (2005) 97–110.
- [14] T. Kitashima, T. Yokokawa, A.C. Yeh, H. Harada, *Intermetallics* 16 (2008) 779–784.
- [15] C. Booth-Morrison, Z.G. Mao, R.D. Noebe, D.N. Seidman, *Appl. Phys. Lett.* 93 (2008) 033103.
- [16] Y. Zhou, Z.G. Mao, C. Booth-Morrison, D.N. Seidman, *Appl. Phys. Lett.* 93 (2008) 171905.
- [17] Y. Amouyal, Z.G. Mao, D.N. Seidman, *Acta Mater.* 58 (2010) 5898–5911.
- [18] Y. Zhou, Z.G. Mao, C. Booth-Morrison, D.N. Seidman, *Appl. Phys. Lett.* 94 (2009) 041917.
- [19] Y.J. Wang, C.Y. Wang, *Mater. Sci. Eng. A* 490 (2008) 242–249.
- [20] Y. Zhou, Z.G. Mao, D.N. Seidman, *Appl. Phys. Lett.* 95 (2009) 161909.
- [21] A. Mottura, N. Warnken, M.K. Miller, M.W. Finnis, R.C. Reed, *Acta. Mater.* 58 (2010) 931–942.
- [22] B.H. Ge, Y.S. Luo, J.R. Li, J. Zhu, *Scripta Mater.* 63 (2010) 969–972.
- [23] T. Zhu, C.Y. Wang, Y. Gan, *Acta. Mater.* 58 (2010) 2045–2055.
- [24] Y. Liu, K.Y. Chen, G. Lu, J.H. Zhang, Z.Q. Hu, *Acta. Mater.* 45 (1997) 1837–1849.
- [25] Y.X. Wu, X.Y. Li, Y.M. Wang, *Acta Mater.* 55 (2007) 4845–4852.
- [26] S. Sanyal, U.V. Waghmare, P.R. Subramanian, M.F.X. Gigliotti, *Scripta Mater.* 63 (2010) 391–394.
- [27] L. Peng, P. Peng, D.D. Wen, Y.G. Liu, H. Wei, X.F. Sun, Z.Q. Hu, *Mater. Sci. Eng.* 19 (2011) 065002.
- [28] K.Y. Chen, L.R. Zhao, J.S. Tse, *Acta. Mater.* 51 (2003) 1079–1086.
- [29] K. Chen, L.R. Zhao, J.S. Tse, *Mater. Sci. Eng. A* 365 (2004) 80–84.
- [30] K. Chen, L.R. Zhao, J.S. Tse, *Mater. Sci. Eng. A* 360 (2003) 197–201.
- [31] X.F. Gong, G.X. Yang, Y.H. Fu, Y.Q. Xie, J. Zhuang, X.J. Ning, *Comp. Mater. Sci.* 47 (2009) 320–325.
- [32] P. Peng, A.K. Soh, R. Yang, Z.Q. Hu, *Comp. Mater. Sci.* 38 (2006) 354–361.
- [33] C. Wang, C.Y. Wang, *Surf. Sci.* 602 (2008) 2604–2609.
- [34] Y.J. Wang, C.Y. Wang, *Scripta Mater.* 61 (2009) 197–200.
- [35] X. Zhang, C.Y. Wang, *Acta. Mater.* 57 (2009) 224–231.
- [36] X.L. Hu, Y. Zhang, G.H. Lu, T. Wang, *J. Phys. Condens. Matter.* 21 (2009) 025402.
- [37] X.L. Hu, L.H. Liu, Y. Zhang, G.H. Lu, T. Wang, *J. Phys.: Condens. Matter.* 23 (2011) 025501.
- [38] Y. Wei, H.B. Zhou, Y. Zhang, G.H. Lu, H. Xu, *J. Phys.: Condens. Matter.* 23 (2011) 225504.
- [39] Y. Wei, Y. Zhang, H.B. Zhou, G.H. Lu, H. Xu, *Intermetallics* 22 (2012) 41–46.
- [40] M.C. Payne, M.P. Teter, D.C. Allan, T.A. Arias, J.D. Joannopoulos, *Rev. Mod. Phys.* 64 (1992) 1045–1097.
- [41] M.D. Segall, P.J.D. Lindan, M.J. Probert, C.J. Pickard, P.J. Hasnip, S.J. Clark, M.C. Payne, *J. Phys. Condens. Matter.* 14 (2002) 2717–2744.
- [42] D. Vanderbilt, *Phys. Rev. B* 41 (1990) 7892–7895.
- [43] J.P. Perdew, K. Burke, M. Ernzerhof, *Phys. Rev. Lett.* 77 (1996) 3865–3868.
- [44] P. Ravindran, G. Subramoniam, R. Asokamani, *Phys. Rev. B* 53 (1996) 1129–1137.
- [45] J.H. Xu, B.I. Min, A.J. Freeman, T. Oguchi, *Phys. Rev. B* 41 (1990) 5010–5016.
- [46] G.P. Francis, M.C. Payne, *J. Phys. Condens. Matter.* 2 (1990) 4395–4404.
- [47] P. Pulay, *Mol. Phys.* 17 (1969) 197–204.
- [48] T.H. Fischer, J. Almlöf, *J. Phys. Chem.* 96 (1992) 9768–9774.
- [49] H. Harada, A. Ishida, H.K.D.H. Bhadeshia, M. Yamazaki, *Appl. Surf. Sci.* 67 (1993) 299–304.
- [50] R.C. Reed, A.C. Yeh, S. Tin, S.S. Badu, M.K. Miller, *Scripta Mater.* 51 (2004) 327–331.
- [51] B.R. Sahu, *Mater. Sci. Eng. B* 49 (1997) 74–78.
- [52] Y.J. Li, Q.M. Hu, D.S. Xu, R. Yang, *Intermetallics* 19 (2011) 793–796.
- [53] K.Y. Chen, L.R. Zhao, J.S. Tse, *Philos. Mag.* 83 (2003) 1685–1698.
- [54] W.T. Geng, A.J. Freeman, R. Wu, C.B. Geller, J.E. Reynolds, *Phys. Rev. B* 60 (1999) 7149–7155.